

**ICSO 2016**

**International Conference on Space Optics**

Biarritz, France

18–21 October 2016

*Edited by Bruno Cugny, Nikos Karafolas and Zoran Sodnik*



***An on-board calibration assembly (OBCA) on the ENMAP satellite***

*Ludger Wilkens*

*Bernhard Sang*

*Markus Erhard*

*Hermann Bittner*

*et al.*



icso proceedings



## AN ON-BOARD CALIBRATION ASSEMBLY (OBCA) ON THE ENMAP SATELLITE

Ludger Wilkens (ludger.wilkens@ohb.de)<sup>1</sup>, Bernhard Sang (bernhard.sang@ohb.de)<sup>1</sup>, Markus Erhard (markus.erhard@ohb.de)<sup>1</sup>, Hermann Bittner (hermann.bittner@ohb.de)<sup>1</sup>, Andreas Grzesik (andreas.grzesik@ohb.de)<sup>1</sup>, Sebastian Eberle (eberle@krp-m.de)<sup>2</sup>, Christoph Bräuninger (cb@braeuninger-konstruktion.de)<sup>3</sup>, Michaela Sornig (manuela.sornig@dlr.de)<sup>4</sup>, Sebastian Fischer (Sebastian.Fischer@dlr.de)<sup>4</sup>

<sup>1</sup>OHB System AG, Germany. <sup>2</sup>KRP-Mechatec Engineering GbR. <sup>3</sup>Bräuninger & Konstruktionen. <sup>4</sup>German Aerospace Center (DLR).

### I. INTRODUCTION

The Environmental Mapping and Analysis Program (EnMAP) is a German hyperspectral satellite mission that aims at monitoring and characterizing the Earth's environment on a global scale. Its hyperspectral imager (HSI) is capable of measuring the solar radiance reflected from the Earth's surface as a continuous spectrum in the spectral range of 420 nm to 2450 nm. The imager operates in a sun synchronous orbit in a height of 653 km with a ground track image swath width of 30 km and a ground sampling distance of 30 m x 30 m. This is achieved by applying an F#3 optical design.

The telescope assembly (TA) is an three mirror anastigmat (TMA) of Wetherell-Womble type. The Instrument Spectrometer Unit (ISU) comprises mainly the two prism spectrometers for the SWIR and the VNIR channel. The spectrometer design is a novel type of compact Offner spectrometers with curved prisms [2].

#### A. Design description of the Instrument Optical Unit (IOU)

The architectural design of the image forming elements of the HSI is shown in Fig. 1.

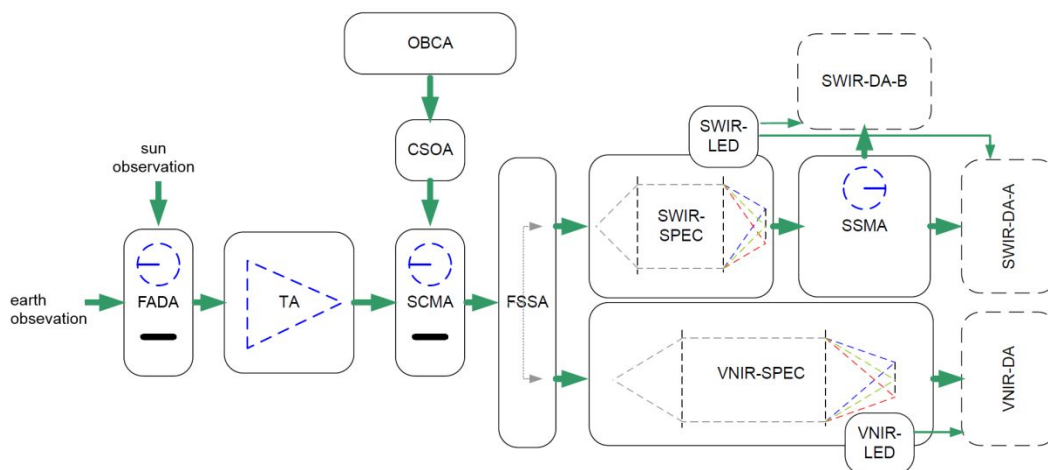


**Fig. 1.** Architectural design of the Telescope Assembly (TA) and the Instrument Spectrometer Unit (ISU).

Light that enters through the entrance aperture of the telescope assembly (TA) is routed to a switching element (Shutter Calibration Mechanism Assembly, SCMA). During earth observation the light passes the SCMA, and the TA forms the image of the ground onto the Field Splitter / Slit Assembly (FSSA). The FSSA acts as the entrance apertures for the spectrometers; it splits and directs the light into the respective VNIR and SWIR spectrometers (VNIR-SPEC and SWIR-SPEC), which create spectrally resolved images of the corresponding entrance slit on the detector assemblies (SWIR-DA and VNIR-DA, respectively). The SWIR channel features a Switch Mirror Assembly (SSMA), that allows to switch once from nominal SWIR-DA-A to redundant SWIR-DA-B detector chains.

#### B In-flight calibration elements

As the radiometric characteristics of the instrument will change between ground and orbit, it has to be calibrated again once it is on the orbit and the calibration needs to be repeated periodically. The HSI contains several sub-systems that allow performing in-flight calibrations and stability checks:

The SCMA has a shutter position, in order to suppress all light from the TA. In this configuration dark signal measurements can be performed.

In front of each detector assembly (VNIR-DA, SWIR-DA-A and SWIR-DA-B) there are LED assemblies mounted outside of the main light path (VNIR-LED and SWIR-LED, see Fig. 1). They are used to characterize the response function of the detectors. During characterization, the main light path is closed by the SCMA. LEDs are switched on and calibration frames are taken with increasing integration times. The corresponding detector readings will be used to calculate a non-linearity correction look-up table (LUT).

The Full Aperture solar Diffuser Assembly (FADA) is used to perform absolute radiometric calibrations and to characterize the response non-uniformity (RNU) of the instrument. During these calibrations the FADA is illuminated by the sun. The diffuser reflects scattered light towards the telescope. Knowing the solar spectral irradiance, one can calculate the calibrating spectral radiance produced by the diffuser.

Finally, the presented On-Board Calibration Assembly (OBCA) generates uniform spectrally broadband light to serve as an intermediate radiometric standard between two sun calibrations. It also provides spatially uniform and spectrally structured light to serve as a spectral reference standard. During these calibrations the SCMA is switched to a mirror position, which reflects light coming from OBCA to the ISU. A Calibration Source Optics Assembly (CSOA) generates an 1:1 image of the output slit of the OBCA onto the spectrometers' apertures (FSSA).

## II. KEY FEATURES OF THE ON-BOARD CALIBRATION ASSEMBLY

### A. Radiometric stability

OBCA shall generate uniform spectrally broadband light to serve as an intermediate radiometric standard between two sun calibrations. It shall provide several (at least 5) adjustable radiance levels of spectrally smooth (white) reference radiance (black body type radiance curve) for checking stability of the HSI radiometric response over the entire spectral range (420 nm - 2450 nm). These radiance levels shall be smaller or equal to the maximal radiance  $L_{\max}$  and higher than the reference radiance  $L_{\text{ref}}$  expected in orbit (shown in Fig 1).

The curves in Fig. 1 show the spectral earth radiance for different solar zenith angles  $\alpha$  and surface reflectance values  $\rho$  ( $L_{\text{ref}}$ :  $\alpha = 30^\circ$ ,  $\rho = 0.3$ ,  $L_{\max}$ :  $\alpha = 0^\circ$ ,  $\rho = 0.9$ ). The envelope of the spectrum can be described by black body radiation at  $T_{\text{BB}} \approx 5900$  K with a maximum at  $\lambda_{\max} \approx 500$  nm.

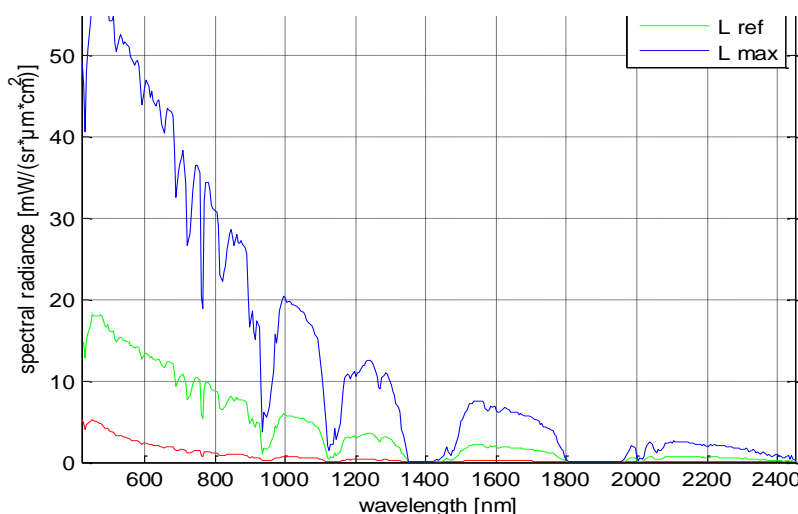


Fig. 2. Spectral earth radiance for different solar zenith angles and surface reflectance values.

The OBCA utilizes two types of light sources: tungsten halogen lamps and white LEDs. Halogen lamps provide broadband illumination, covering the whole spectral range of EnMAP. In first approximation the lamps can be described as black body radiators with  $T_{\text{BB}} \approx 3000$  K and  $\lambda_{\max} \approx 900$  nm.

Since the color temperature of the halogen lamp (3000 K) is relatively low compared to the sun, the shorter part of the spectrum sharply declines in the intensity, creating deficit of the useful signal in the blue region. In order to enhance energy level in this region the white LED is applied (blue LED with phosphor layer). The peak wavelength of the blue LED is at 450 nm, the peak wavelength of the phosphor at 555 nm.

The angular homogeneity in the F#3 cone over the aperture shall be better than 90 %, the spatial homogeneity shall be better than 95 %.

The angular and spatial homogeneity will be realized by placing the light sources into an integrating sphere. The sphere is covered with polytetrafluoroethylene (PTFE) diffuser material, which provides a spectrally broad, white spectrum of reflection: the reflectivity of the white diffuser material named Spectralon® is higher than 95% in spectral range 420-1600 nm and higher than 90% above 1600 nm.

It is known that the reflectance of Spectralon degrades when exposed to UV and VUV. This degradation is most significant in the short wavelength region, where the reflectance decreases noticeably. Investigations have shown that the degradation is caused by volatile contaminants deposited in the PTFE [1]. A procedure for production and handling of Space Grade Spectralon has been established by Labsphere (the manufacturer of the Spectralon® parts) in order to overcome this degradation. Therefore, the Spectralon® parts that are used for the OBCA were manufactured according to these Space Grade best practices.

Radiance levels for radiometric stability shall be repeatable for two consecutive calibrations within 2 %. As the spectral fluxes of all used light sources are temperature dependent (in particular the integral flux of the LEDs), the temperature of the light sources must be controlled.

### B. Spectral stability

The OBCA also provides light with prominent spectral features in order to serve as a spectral reference standard for determining shifts in HSI spectral alignment. The spectral characteristics of the instrument are periodically verified in order to detect these spectral shifts and to correct the instrument optical model and data processing algorithm, if necessary.

The spectral reference radiance has at least three clearly identifiable features within each spectral channel (VNIR: 420 nm - 1000 nm and SWIR: 900 nm - 2450 nm, resp.).

The spectrally structured light is realized by a second integrating sphere that serves as a light source for the large sphere. It is made of doped diffuser material (Spectralon®) and equipped with halogen lamps.

Doped Spectralon® is commonly used for wavelength calibration standards, covering the UV-VIS-NIR region. The wavelength standards are realized by impregnating Spectralon® with the oxides of rare earth elements, which display sharp absorption spikes at specific wavelengths (see Fig. 3). Three different lanthanide oxides are used: Holmium oxide  $\text{Ho}_2\text{O}_3$  for UV-VIS-NIR calibrations, dysprosium oxide  $\text{Dy}_2\text{O}_3$  for NIR calibration and Erbium oxide  $\text{Er}_2\text{O}_3$  for VIS-NIR calibrations. The Spectralon Multi-Component Wavelength Calibration Standard (WCS-MC) combines the three rare earth oxides.

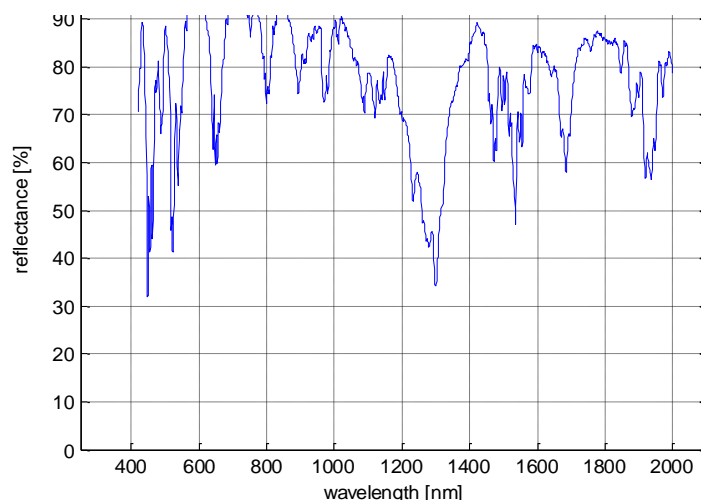


Fig. 3. Reflectance spectra of doped Spectralon WCS-MC

### III. GENERAL DESIGN OF THE OBCA

The general design of the OBCA is sketched in Fig. 4. The assembly comprises two integrating spheres equipped with a number of light sources. The inner surface of the big sphere is made out of white Spectralon. Two halogen lamps (prime Lamp\_1R and redundant Lamp\_2R) and one LED (LED\_C) can illuminate the sphere. During radiometric stability measurements only one of the two halogen lamps is operated together with the LED; the second lamp is added as a redundancy, in case the first lamp fails.

Close to the LED there is a Loop Heat Pipe interface (LHP I/F) that will be connected to a loop heat pipe, in order to control the temperature of the LEDs. Three thermal sensors ((1), (2) and (3) in Fig. 5) monitor the temperature of the LHP I/F, the LED and the halogen lamps.

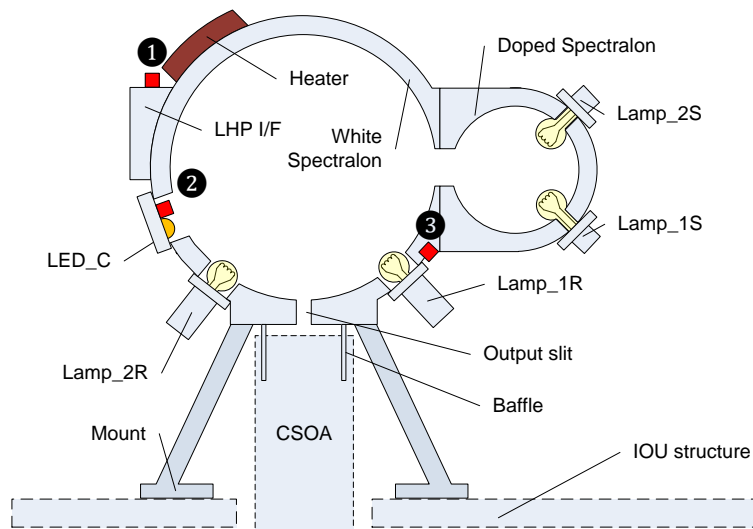


Fig. 4. General design of the OBCA

The small sphere – made out of doped Spectralon® - serves as a light source for the large sphere. Like the big sphere it is equipped with two halogen lamps (prime Lamp\_1S and redundant Lamp\_2S). During spectral stability checks only one of the two halogen lamps is operated. Again, the second lamp is added for redundancy.

It has to be mentioned that there are twice as many light sources at the OBCA because the EnMAP reliability concept foresees a second electrical circuit, independent from the nominal one, in case the nominal circuit fails for any reason. This means that every light source shown in Fig. 4 is mirrored by a redundant counterpart.

The OBCA output port is imaged by the calibration optics assembly (CSOA) onto the FSSA. The OBCA is not in physical contact with the CSOA. However, a labyrinth type light trap interface design in-between the two baffles of CSOA and OBCA ensures light tightness to a very high degree. The surfaces of the baffle and the output slit are coated black (Acktar Fractal Black®) for straylight reduction.

The OBCA is thermally isolated from the IOU structure by a light weighted mount and spherical washers.

## V. DESIGN MATCHING BETWEEN THE OBCA STRUCTURE AND THE LAMPS

A key design driver was the design matching between the OBCA structure and the lamps with respect to the eigenmodes. Early vibration tests have shown that the filaments of the lamps can break at relatively low load levels. Therefore, a detailed investigation on different halogen lamps was necessary.

### A. Evaluation of halogen lamps

The search for halogen lamps was restricted by design limitations (the component should ideally fit in a G4 lamp adapter). In addition, the nominal power had to be approximately 10W. Smaller lamps do not provide the required spectral flux; more powerful lamps need to be operated at low currents (which leads to an undesirable shift of  $\lambda_{max}$  to higher wavelengths; besides, permanent dimming can also reduce the life time of the lamps). Two types of OSRAM lamps were evaluated: *Halostar Starlite 64415 S* (low-voltage halogen lamps with G4 pin base and axial filament; 10 W nominal wattage) and *Halostar Standard 64415 ND* (Specification similar to *Halostar Starlite*, but with vertical filament).

Both lamps were tested regarding their limit loads. The lamps, mounted in their lamp holders, were attached to an aluminum test adapter, which provided all different lamp orientations in x, y and z axis (for definition of lamp orientation see Fig. 5). The assembly was tested with random phase excitation. The excitation spectrum was defined by the envelope of the single axes' qualification load spectra. The spectrum was applied with increasing loads (1 dB steps) starting with qualification level. After each step the lamps were checked for proper operation.



Fig. 5. Definition of the lamp orientation

As a result it can be stated that only for z direction of the *Halostar Standard* the shaker limit was reached before any failure. In all other directions both lamps types showed failures caused by a broken filaments. The limit loads (i.e. the last survived load levels) are listed in Table 1. Compared to the *Halostar Starlite* the limit loads of the *Halostar Standard* were substantially higher in 2 of 3 directions, in x direction the first failure occurred one test step earlier.

Table 1. Summary of limit load test results ( $1\sigma$  values).

Local lamp orientation	Starlite 64415 S		Standard 64415 ND	
	Survived load level	Level of first failure	Survived load level	Level of first failure
	grms [g]	grms [g]	grms [g]	grms [g]
x	35.34	39.65	31.24	35.09
y	17.81	19.97	27.48	31.24
z	39.65	44.14	49.21	N/A

The resonant frequencies of the halogen lamps were measured at the *Environmental Simulation Laboratory* of OSRAM. 10 lamps of both type were measured in each direction. Result are shown in Table 2.

The eigenfrequencies of the *Halogen Standard* are at lower frequencies; the gap between the first 2 frequencies is smaller than for the *Halostar Starlite* (65 Hz vs. 130 Hz).

Table 2. Summary of resonant frequency measurements.

Lamp Type	1st eigenfrequency $f_1$ (y direction)	2nd eigenfrequency $f_2$ (x direction)
Starlite 64415 S	450 Hz	580 Hz
Standard 64415 ND	430 Hz	495 Hz

For both types of lamps a stability test was carried out for 5 lamps each. During that test the lamps were operated for 300 hours at nominal power. Prior to the 300 hours operation and afterwards the spectral flux was measured for each lamp. The measurements showed that the *Halostar Standard* were qualitatively inferior to the *Halostar Starlite*, with respect to the stability of the integrated spectral flux after the 300 hours operation.

To decide, which of the both lamp types is more suitable for the OBCA, one must have a deeper look at the OBCA structure and its structural behavior.

### B. Optimization of the OBCA structure

A vibration test was performed - using a representative OBCA model - in order to measure the eigenfrequencies of the OBCA and to correlate the FE model of the structural analysis with the test results. The aluminum shell, the steel mount and Spectralon® parts were identical in construction to the flight model. Lamp dummies were used instead of the light sources (see Fig. 6). A sine search and a random vibration test were performed in that test.

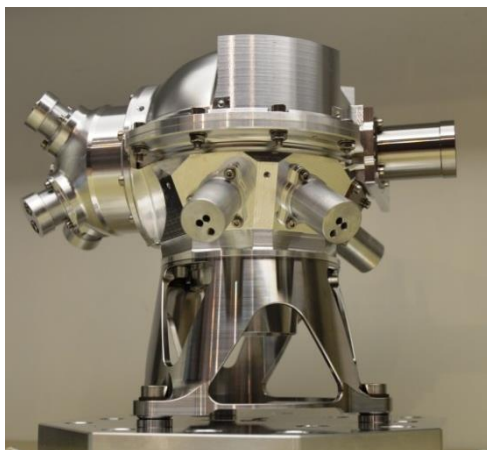


**Fig. 6.** OBCA dummy for vibration test

The test showed that the 1<sup>st</sup> eigenfrequency of the OBCA was at 480 Hz (bending mode, “small sphere’s head nod”), the 2<sup>nd</sup> eigenfrequency at 500 Hz (bending mode, ”small sphere’s head shake”). Comparing these frequencies with the resonant frequencies of the lamps (Table 2) one sees that they are very close. A decoupling of the eigenfrequencies of the OBCA and the lamps is necessary.

Variations of the mount of the OBCA – i.e. a less stiff design with modified interfaces to IOU structure and aluminum shell, different materials (titan instead of steel) and wall thicknesses (2.5 mm instead of 3.5 mm) – were designed and analyzed, in order to reduce the stiffness and to optimize the eigenfrequencies. The results of these variations are shown in Table 3.

The desired lamp decoupling of the two first OBCA modes can only be achieved by changing the mount material and wall thickness, as well as the design at the interfaces. One drawback of a modified design is that an 3<sup>rd</sup> torsional eigenmode arises close to the lamps eigenmodes.

**Table 3.** resonant frequencies of several OBCA variations.

	<b>Interface-Design</b>	<b>Wall thickness</b>	<b>Mount material</b>	<b>1st bending mode [Hz]</b>	<b>2nd bending mode [Hz]</b>	<b>Torsional mode [Hz]</b>
Test mount	Original	3.5 mm	Steel	480	500	732
Variation #1	Original	3.5 mm	Ti	424	442	661
Variation #2	Original	2.5 mm	Ti	407	418	643
Variation #3	Alternative	3.5 mm	Ti	358	379	560
Variation #4	Alternative	2.5 mm	Ti	317	335	471

A variation of the mount not only changes the eigenmodes, but also the acceleration at the position of the lamps. The highest accelerations occur at the upper lamps of the small sphere (see Fig. 6). Table 4 shows the variation of the integrated loads  $A$  at the lamp holder position in a random environment.  $A_x$ ,  $A_y$  and  $A_z$  denote the local coordinate systems of the lamps, The loads are in grms ( $1\sigma$ ). One sees that the load on the lamp holder increases with decreasing the mount stiffness.

**Table 4.** Maximum acceleration at lamp holder position for several OBCA variations.

	<b>Interface-Design</b>	<b>Wall thickness</b>	<b>Mount material</b>	<b><math>A_x</math> [grms]</b>	<b><math>A_y</math> [grms]</b>	<b><math>A_z</math> [grms]</b>
Test mount	original	3.5 mm	Steel	11.4	12.2	10.5
Variation #1	Original	3.5 mm	Ti	15.6	15.3	13.2
Variation #2	Original	2.5 mm	Ti	17.7	16.3	14.7
Variation #3	alternative	3.5 mm	Ti	22.3	18.1	17.2
Variation #4	alternative	2.5 mm	Ti	28.7	23.9	20.8

The results in Table 4 neglect the coupling between the OBCA modes and the lamp filaments. In order to evaluate this effect, the dynamic behavior of the filaments is included in the model in the form of a mass-spring

system on the top of the modeled lamp. For the mass of the filament we assume  $m_{filament} = 4.2$  mg. To determine the required stiffness of the mass-spring system  $k_i$  ( $i = x, y$ ), the following equation was used:

$$k_i = (2 \pi \cdot f_i)^2 \cdot m_{filament}, \tag{1}$$

with  $f_i$  ( $i = 1, 2$ ) the first two resonant frequencies of the respective lamp (see Table 2). With the resulting values for  $k_i$  the analysis was performed. The results are shown in Table 5. The *Halogen Starlite* decoupled on average better than the *Halogen Standard*. The decoupling is clearly best for the mount with the alternative design and the reduced wall thickness.

**Table 5.** Maximum acceleration at lamp filament for several OBCA variations ( $1\sigma$  values).

	Starlite 64415 S			Standard 64415 ND		
	A <sub>x</sub> [grms]	A <sub>y</sub> [grms]	A <sub>z</sub> [grms]	A <sub>x</sub> [grms]	A <sub>y</sub> [grms]	A <sub>z</sub> [grms]
Test mount	88.6	39.7	10.8	55.4	181.7	10.8
Variation #1	271.0	330.	13.5	246.8	64.6	13.5
Variation #2	133.4	32.6	15.0	262.5	54.2	15.0
Variation #3	78.7	33.6	17.5	103.9	45.0	17.3
Variation #4	70.0	40.9	21.0	76.2	47.7	21.0

In the next step the different limit loads of the two lamps are taken into account. To estimate the criticality of the loads of the two different lamp types, the loads in the areas of the eigenmodes of the lamps (in a 1/3 octave interval) were integrated for the limit load level, i.e. the last level where all lamps survived the vibration test (*Starlite 64415 S*: 6dB, *Standard 64415 ND*: 10dB). The loads and frequency ranges are shown in Table Fig. 7 for both lamps (left side: *Halostar Starlite*, right side: *Halostar Standard*).

**Table 6.** Limit loads  $A_{Lamp,i}$  for the first 2 eigenmodes ( $i=1,2$ ) in the 1/3 octave intervals ( $1\sigma$  values).

		Starlite 64415 S		Standard 64415 ND	
		f <sub>1</sub>	f <sub>2</sub>	f <sub>1</sub>	f <sub>2</sub>
Frequency	[Hz]	450	580	431	495
1/3 octave integral $A_{Lamp,i}$	[grms]	6.43	4.92	9.98	10.03

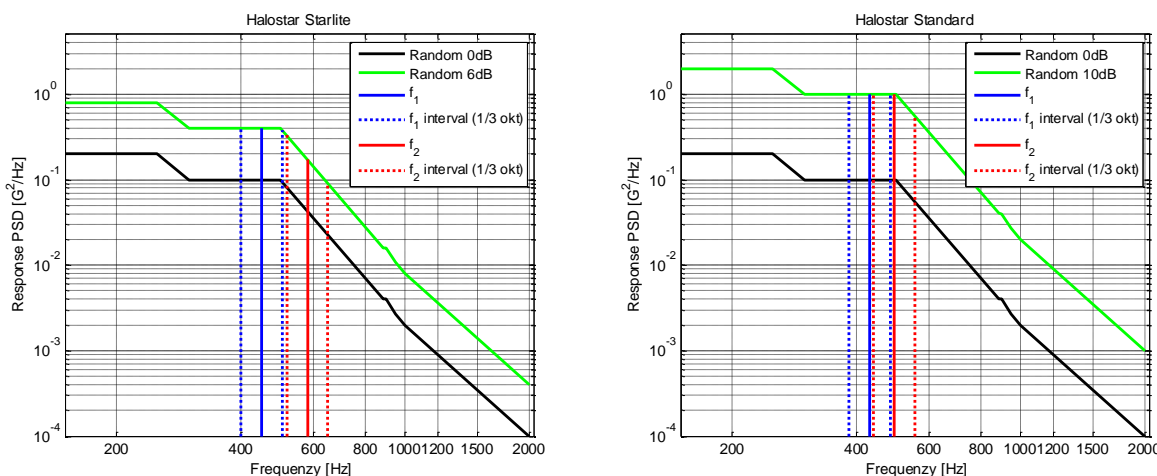


**Fig. 6.** 1/3 octave intervals for the first two eigenmodes.

For the 5 featured OBCA designs the input loads  $A_{OBCA,i}$  were calculated for the highest loaded lamps (the upper lamps of the small sphere) for the 1/3 octave eigenfrequency intervals  $i$  ( $i=1,2$ ) shown in Fig. 6. To prevent failure, input loads  $A_{OBCA}$  must be smaller than the respective limit loads  $A_{Lamp}$  for both eigenmodes (including a factor of safety of 1.5). Comparing the input loads with the limit loads one sees that only when the first resonant frequency of OBCA is as low as 380 Hz, there is a positive margin between this loads, independent of the choice of the lamps.

For the choice for the final configuration it has been taken into account that:

- a 50% margin in the 1/3 octave analysis shall be considered as sufficient
- In terms of OBCA coupling with the lamp filaments the *Halostar Starlite* is slightly advantageous for OBCA variations with low eigenfrequencies.
- In terms of radiometry the *Halostar Starlite* is preferred, due to a higher stability

Considering the results of 1/3 octave analysis, the OBCA coupling with the lamp filaments and the higher radiometric stability of the *Halostar Starlite*, this lamp and a Titan Mount with the first eigenfrequency at about 380 Hz is chosen for the final design.

The reduction of the resonant frequencies were realized by reducing the wall thickness of the mount, designing thinner feet (with a smaller diameter) and foreseeing larger cutouts on the struts, as shown in Fig. 7.

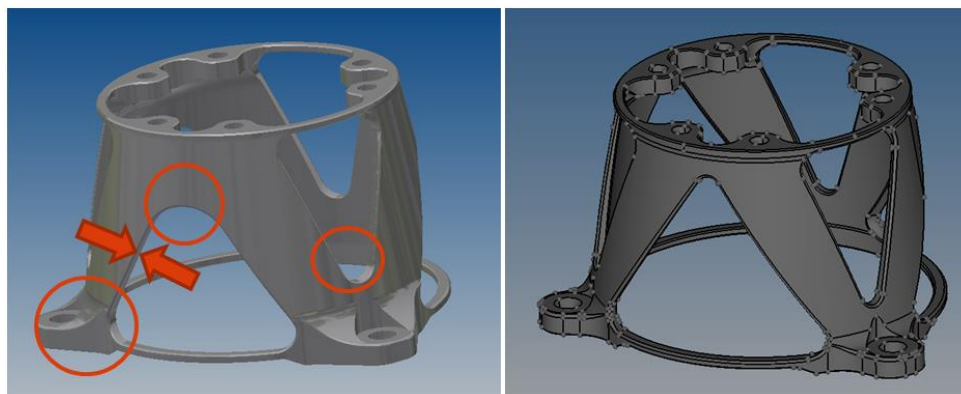


Fig. 7. Design changes of the OBCA mount

## VI. CONCLUSION

In this paper we introduced the On-Board Calibration Assembly (OBCA) that is used as a calibration source at German hyperspectral satellite mission EnMAP. A design description of the instrument's optical unit was given, in particular the in-flight calibration elements.

The OBCA operates in either of two modes: radiometric and spectral calibration mode. In radiometric mode, it generates uniform broadband light to serve as an intermediate radiometric standard. In spectral mode, it provides spatially uniform, spectrally structured light to serve as a spectral reference standard

The key features of the OBCA were presented: a large integrating sphere made of a white diffuser material, equipped with tungsten halogen lamps and white LEDs that provide broadband illumination, is dedicated for radiometric stability measurements. A small sphere made of doped diffuser, equipped only with halogen lamps, serves as a light source for the large sphere and provides reference signal with a number of stable features for spectral stability check.

A key design driver was the design matching between the OBCA structure and the lamps. Vibration tests have shown that the filaments of the lamps can break at relative low load levels. A decoupling of the eigenfrequencies of the OBCA and the lamps was necessary. Different types of lamps were tested, regarding their limit loads, eigenfrequencies and spectral stability. The design of the OBCA mount has been optimized with respect to stiffness and eigenfrequencies, in order to minimize the load level in the critical frequency ranges. A 1/3 octave model has successfully been established in order to benchmark the survival chance of a given mount-lamp-combination for a given load environment.

The work presented in this paper was performed on behalf of the German Space Agency DLR with funds of the German Federal Ministry of Economic Affairs and Technology under the grant No. 50 EP 0801. The authors are responsible for the contents of this publication.

## REFERENCES

- [1] A.E. Stiegman, C.J. Bruegge, A.W. Springsteen, "Ultraviolet stability and contamination analysis of Spectralon diffuse reflectance material," *Opt. Eng.* 32(4), pp. 799-804, 1993
- [2] B. Sang, J. Schubert, S. Kaiser, V. Mogulsky, C. Neumann, K.P. Förster, et al. "The EnMAP hyperspectral imaging spectrometer: Instrument concept, calibration, and technologies," *Proc. SPIE* 2008, 7086, doi:10.1117/12.794870.